

# FloodSQL-Bench: A Retrieval-Augmented Benchmark for Geospatially-Grounded Text-to-SQL

Hanzhou Liu, Kai Yin, Zhitong Chen, Chenyue Liu, Ali Mostafavi  
Texas A&M University

## Abstract

Existing Text-to-SQL benchmarks primarily focus on single-table queries or limited joins in general-purpose domains, and thus fail to reflect the complexity of domain-specific, multi-table and geospatial reasoning. To address this limitation, we introduce FLOODSQL-BENCH, a geospatially grounded benchmark for the flood management domain that integrates heterogeneous datasets through key-based, spatial, and hybrid joins. The benchmark captures realistic flood-related information needs by combining social, infrastructural, and hazard data layers. We systematically evaluate recent large language models with the same retrieval-augmented generation settings and measure their performance across difficulty tiers. By providing a unified, open benchmark grounded in real-world disaster management data, FLOODSQL-BENCH establishes a practical testbed for advancing Text-to-SQL research in high-stakes application domains.

## 1 Introduction

Text-to-SQL translates natural language questions into executable SQL queries, enabling intuitive access to relational databases through conversational interfaces (Katsogiannis-Meimarakis and Koutrika, 2023). General-purpose benchmarks such as Spider (Yu et al., 2018) and BIRD (Li et al., 2023) have significantly advanced research on this task. However, these benchmarks primarily emphasize single-table queries or simple joins in open-domain settings, and thus fail to capture the challenges of domain-specific, multi-table and geospatial reasoning that are crucial for real-world applications.

Flood management is one such domain, where decision-making depends on integrating different data sources, including geographic features, demographic statistics, and critical infrastructure records (Cutter et al., 2012; Wing et al., 2018). Unlike open-domain settings, practitioners must

combine information across multiple layers, for example linking census tracts with floodplain boundaries or associating hospitals with historical flood claims. To overcome these challenges, we propose FLOODSQL-BENCH, a novel benchmark constructed from real-world datasets and designed around progressively complex queries, ranging from single-table lookups to multi-table reasoning involving key-based joins, spatial joins, and their hybrids. This design enables systematic evaluation of Text-to-SQL models on realistic geospatial and socio-economic reasoning tasks essential for flood risk assessment and emergency response.

We evaluate FLOODSQL-BENCH across a diverse set of large language models (LLMs), including both proprietary and open-source variants, under the same retrieval-augmented generation (RAG) settings. Beyond broad model coverage, we further compare model performance across the benchmark’s difficulty tiers to assess how well different LLMs handle increasing levels of schema complexity, table interactions, and geospatial operations.

This work makes the following contributions:

- We introduce FLOODSQL-BENCH, the first Text-to-SQL benchmark tailored to flood-risk analytics, featuring multi-table queries with geospatial reasoning.
- We provide a comprehensive evaluation of multiple LLMs under RAG settings, systematically comparing their performance across difficulty levels ranging from single-table lookups to triple-table spatial-spatial joins.
- Our study shows that while LLMs can handle simple queries reasonably well, they exhibit substantial degradation on complex multi-table and geospatial queries, highlighting the need for structured, metadata-driven, and domain-aware methods.

## 2 Related Work

**Text-to-SQL** research has evolved from single-table parsing to cross-domain and multi-table reasoning. Early datasets such as ATIS and GeoQuery focused on domain-specific grammars, whereas Spider (Yu et al., 2018) established a large-scale cross-domain benchmark that has become the de facto standard for evaluating Text-to-SQL systems. Subsequent works, including SParC (Yu et al., 2019b) and CoSQL (Yu et al., 2019a), extended Spider to multi-turn and conversational settings. More recently, benchmark efforts such as TableBench (Wu et al., 2025) target broader table-based reasoning beyond SQL generation. However, all of these benchmarks primarily center on open-domain databases with relatively simple join structures, and rarely address domain-specific, multi-table reasoning that involves heterogeneous relational and spatial data, a key challenge for high-stakes applications such as flood risk management.

**Geospatial reasoning** introduces unique challenges beyond conventional relational semantics, as queries often involve spatial joins, coordinate transformations, and topology-aware aggregation. Prior work on natural-language interfaces to spatial databases (Li et al., 2019; Liu et al., 2025) and spatial question answering (Chen et al., 2021) has explored spatial relations such as containment, intersection, and proximity. However, these systems are typically evaluated on synthetic or small-scale datasets and do not address realistic, domain-specific reasoning that integrates heterogeneous spatial and tabular information. In contrast, real-world flood management requires the fusion of diverse geospatial sources—such as physical floodplains, demographic indicators, and critical infrastructure layers, to support actionable decision-making (Cutter et al., 2012; Wing et al., 2018). Despite their importance, no existing Text-to-SQL or QA benchmarks systematically incorporate such spatially grounded, multi-table reasoning tasks. FLOODSQL-BENCH bridges this gap by providing a unified benchmark that combines key-based, spatial, and hybrid joins across real disaster-management datasets, enabling rigorous evaluation of large language models (LLMs) under retrieval-augmented (RAG) settings.

**Retrieval-Augmented Generation (RAG)** has become a central approach for grounding large language models (LLMs) in traditional NLP tasks

like question answering and conversation (Lewis et al., 2020; Izacard and Grave, 2021; Shuster et al., 2021), with recent work extending retrieval beyond unstructured text to structured sources such as relational databases and tables (Ayala and Bechard, 2024; Wu et al., 2024). However, existing text-to-SQL benchmarks primarily focus on non-spatial schema and do not evaluate reasoning over geometric data, spatial joins, or multi-layer geospatial infrastructures. Although prior work has explored geospatial question answering using knowledge graphs (Li et al., 2025) and GIS tool-driven workflow automation (Zhang et al., 2024), neither line of research concentrates on SQL-based spatial joins across multiple tables. Recent advances in table-aware retrieval (Zhang et al., 2023; Ziletti and DAmbrosi, 2024) further highlight the importance of retrieval granularity for structured reasoning, yet these methods have not been explicitly tested in spatial settings where geometry, topology, and coordinate systems must be considered. To the best of our knowledge, FLOODSQL-BENCH addresses these gaps by providing the first benchmark designed for multi-layer geospatial SQL reasoning and RAG evaluation, enabling systematic assessment of LLMs across lookup, relational, and spatially grounded analytical queries.

## 3 Benchmark Construction

To balance realism with tractability, FLOODSQL-BENCH focuses on three flood-prone states, Texas, Florida, and Louisiana, which together account for a disproportionate share of National Flood Insurance Program (NFIP) claims and Federal Emergency Management Agency (FEMA)-declared disasters. Within this scope, FLOODSQL-BENCH integrates ten heterogeneous tables across three spatial aspects: (i) non-spatial layers, claims, svi<sup>1</sup>, cre<sup>2</sup>, nri<sup>3</sup>; (ii) polygon layers, floodplain, census\_tracts, zcta, county; and (iii) point layers, schools, hospitals. These layers reflect key information needed for flood risk management (Cutter et al., 2012; Wing et al., 2018).

All external datasets used in the proposed benchmark FLOODSQL-BENCH are sourced from publicly accessible U.S. government open-data portals, including datasets provided by U.S. Census Bureau, FEMA, CDC/ATSDR, and HIFLD, encom-

<sup>1</sup>svi: Social Vulnerability Index.

<sup>2</sup>cre: Community Resilience Estimates.

<sup>3</sup>nri: National Risk Index.

|       | Tract | Flood | ZCTA | Schl | Hosp | Claim | Cnty | NRI | SVI | CRE |
|-------|-------|-------|------|------|------|-------|------|-----|-----|-----|
| Tract | —     | S     | S    | S    | S    | K     | S/K  | K   | K   | K   |
| Flood | S     | —     | S    | S    | S    | .     | S    | .   | .   | .   |
| ZCTA  | S     | S     | —    | S    | S    | .     | S    | .   | .   | .   |
| Schl  | S     | S     | S    | —    | K    | .     | S    | .   | .   | .   |
| Hosp  | S     | S     | S    | K    | —    | .     | S/K  | .   | .   | .   |
| Claim | K     | .     | .    | .    | .    | —     | K    | K   | K   | K   |
| Cnty  | S/K   | S     | S    | S    | S/K  | K     | —    | K   | K   | K   |
| NRI   | K     | .     | .    | .    | .    | K     | K    | —   | .   | .   |
| SVI   | K     | .     | .    | .    | .    | K     | K    | .   | —   | .   |
| CRE   | K     | .     | .    | .    | .    | K     | K    | .   | .   | —   |

Table 1: Join relationships among the ten tables in FLOODSQL-BENCH. **S** = spatial join; **K** = key-based join; **S/K** = both spatial and key paths are supported; **—** self. The lower triangle mirrors the upper and is shaded in gray.

passing demographic, infrastructure, hazard, and social-vulnerability data layers.

### 3.1 Tabular Data Foundations

**Geographic Identifiers.** FLOODSQL-BENCH adopts standardized geographic identifiers defined by the U.S. Census Bureau to ensure consistent key-based joins across heterogeneous tables (U.S. Census Bureau, 2020). At the tract level, an 11-digit GEOID encodes a 2-digit state code, a 3-digit county code, and a 6-digit tract code, serving as the primary join key among the `census_tracts`, `claims`, `svi`, `nri`, and `cre` tables. At the county level, the 5-digit prefix of the tract GEOID uniquely identifies each county in the county and hospitals tables. At the ZIP level, the ZIP field serves as the geographic identifier for the schools and hospitals tables. Two spatial layers, `zcta` and `floodplain`, lack non-spatial join keys and are instead linked through spatial relationships only.

**Spatial representation.** FLOODSQL-BENCH standardizes spatial representations across various data sources. Specifically, polygon layers retain geometries to support polygon–polygon joins via spatial SQL functions such as `ST_Intersects`, `ST_Contains`, and etc. In contrast, point layers store only explicit latitude and longitude (LAT&LON) fields, with geometries constructed on demand using `ST_Point(LON, LAT)`. To ensure efficiency, all geometries are projected to a common coordinate reference system (CRS) (Goodchild, 1992; Burrough et al., 2015) and simplified with topology-preserving tolerances (Visvalingam and Whyatt, 2017; GEOS Development Team).

### 3.2 Join Semantics and Relations

FLOODSQL-BENCH defines a unified set of join rules to ensure interpretable query semantics across all ten tables. All joins fall into two major categories, *key-based joins* and *spatial joins*. Key-based joins rely on standardized identifiers such as GEOID, COUNTYFIPS, and ZIP, enabling equality-based connections between non-spatial tables or between attribute tables and administrative layers. Specifically, tract-level 11-digit GEOIDs link claims, census\_tracts, svi, nri, and cre, while the 5-digit prefix of GEOIDs serves as county-level identifiers connecting to the county and schools tables. In addition, ZIP codes bridge schools and hospitals. Spatial joins, by contrast, operate on geometry relationships, following two subtypes, *point–polygon* and *polygon–polygon*. Point–polygon joins associate schools or hospitals with surrounding spatial layers (`census_tracts`, `floodplain`, `zcta`, and `county`) through their LAT/LON coordinates. Polygon–polygon joins capture geometric overlaps among regional layers, including intersections between `floodplain`, `census_tracts`, `zcta`, and `county`. Together, these 14 key-based and 14 spatial join rules form the core relational backbone of FLOODSQL-BENCH, enabling a wide range of key-based, spatial, and hybrid SQL queries. A summary of all join pairs is presented in Table 1.

### 3.3 Metadata Builder

In a cross-table benchmark such as FLOODSQL-BENCH, metadata is not merely supplementary documentation but an integral component of the retrieval-augmented generation (RAG) framework

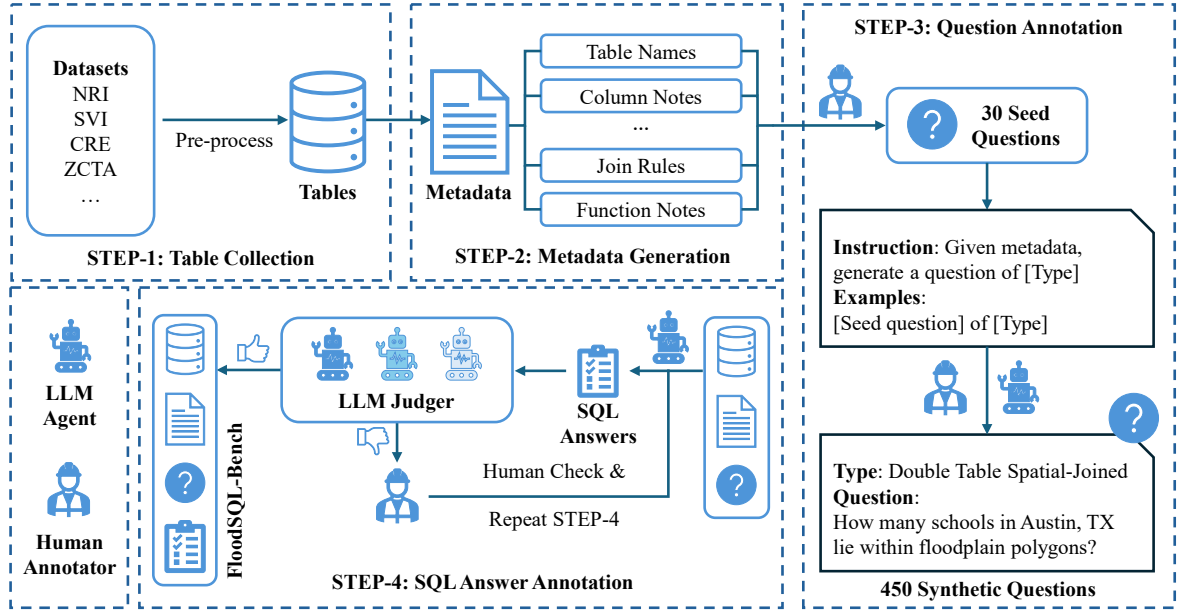


Figure 1: A simplified overview of the annotation framework of our proposed FLOODSQL-BENCH.

itself. Without a structured metadata schema, it would be infeasible to construct a reliable RAG system capable of reasoning over heterogeneous tables. Accordingly, we design an enriched metadata schema that extends beyond basic table and attribute names, serving as the connective layer that bridges schema understanding and natural-language retrieval. It includes detailed field descriptions, data types, sample entries, join rules, function annotations, and supplementary notes, providing the semantic grounding necessary for accurate multi-table retrieval and reasoning.

### 3.4 Question and SQL Annotation

Figure 1 illustrates the simplified progress of annotating FLOODSQL-BENCH. Each question–SQL pair in FLOODSQL-BENCH is designed to reflect realistic analytical needs in flood management. We construct natural language questions based on the underlying spatial and relational structure of the datasets, ensuring that each query is executable and grounded in real-world semantics. All SQL queries are verified for correctness, and corresponding question texts are reviewed to balance linguistic diversity with structural clarity. Table 2 showcases sample questions with specific question types.

**Question Annotation.** FLOODSQL-BENCH emphasizes diverse spatial and hybrid reasoning patterns that reflect real analytical workflows in flood risk assessment, rather than focusing solely on relational operations. To balance coverage and com-

plexity, we organize 443 questions into six categories according to the number and type of joins involved, which are shown in Table 2. This taxonomy captures the increasing difficulty from single-table lookups to triple-table geospatial reasoning, providing a structured foundation for evaluating model performance across progressively complex geospatial tasks. Table 2 reports the question categories, number of samples, description, and example questions in each category.

We follow the procedure of TableBench (Wu et al., 2025) to construct diverse question–SQL pairs. Specifically, we first manually design five seed questions for each category, covering representative reasoning patterns. Next, we parse both the metadata and seed questions into the LLM agent, which automatically expand them into a larger set of candidate questions. We then conduct a human review process to ensure quality and diversity, where annotators limit the frequency of specific tables, attributes, and operations (e.g., aggregation, area computation, TOP–k queries, “best” selection, or location comparison). Finally, each question is manually rewritten for clarity and naturalness, ensuring that it remains human-readable and provides sufficient semantic hints for both human annotators and LLM agents to generate executable SQL. Next, we describe the procedure used to construct the gold SQL answers in a fair and consistent way.

**SQL Annotation.** We employ an LLM agent to generate SQL queries under strict schema and func-

| Level | # of Tables | Join Types      | Example Question  | Sample Question Type  |
|-------|-------------|-----------------|---|---|
| L0    | 1           | None            | <p>1) Return the fraction (0–1) of Texas census tracts where the estimated percent of population with no Internet access is greater than 20%.</p> <p>2) Return the number of NFIP claims in Texas (identified by GEOID starting with 48) with zero insurance payout amount (in USD) for Increased Cost of Compliance (ICC).</p> <p>3) Return the average non-null annual frequency of riverine flood events in Texas (identified by GEOID starting with 48).</p>  | <p>1) fraction computation</p> <p>2) filter and count</p> <p>3) average computation</p>   |
| L1    | 2           | Key             | <p>1) Which non-null year had the highest total number of NFIP flood claims in Louisiana (STATEFP 22), based on a key-based join between claims and county tables? Return the year.</p> <p>2) Return the average non-null Normalized coastal flood risk score among unique Texas tracts (STATEFP 48) that have NFIP claims after 2000-01-01 and non-null NRI risk scores.</p> <p>3) How many non-null ZIP codes in Florida (STATEFP 12) contain both at least one school and one hospital?</p>  | <p>1) maximized aggregation and temporal ranking</p> <p>2) average computation and multi-criteria filter</p> <p>3) intersection filter and distinct count</p> |
| L2    | 2           | Spatial         | <p>1) How many schools in San Antonio, TX (identified by CITY = 'SAN ANTONIO' and STATEFP = '48') fall inside floodplain polygons?</p> <p>2) Which census_tract in Hillsborough County, FL (identified by STATEFP = '12' and COUNTYFP = '057') has the largest total overlap area with all zcta polygons? Return its 11-digit GEOID.</p> <p>3) How many pairs of census_tracts in Hillsborough County, FL (STATEFP = '12' and COUNTYFP = '057') share a common boundary?</p>  | <p>1) point-in-polygon counting</p> <p>2) area-overlap ranking</p> <p>3) boundary-adjacency counting</p>  |
| L3    | 3           | Key-Key         | <p>1) Which 3 Texas counties (STATEFP 48) have the highest total non-null NFIP building payouts weighted by the non-null historical loss ratio for buildings due to coastal flooding? Return their county names.</p> <p>2) In Harris County, TX (GEOID 48201), among tracts that have NFIP claims, what is the average non-null expected annual coastal flood loss per capita based on SVI total population?</p> <p>3) List the 5 Texas (STATEFP 48) census tracts with the highest ratio of NRI riverine expected annual building loss to total housing units among tracts with NFIP claims.</p>   | <p>1) weighted aggregation and ranking</p> <p>2) per-capita metric computation</p> <p>3) ratio computation and top-k selection</p>                            |
| L4    | 3           | Key-Spatial     | <p>1) For Louisiana (STATEFP 22), which 5 counties contain the largest number of schools located in floodplain areas?</p> <p>2) For Florida (STATEFP 12), what is the average relative percentile rank for Summary percentile rank for Theme 1 across all census tracts that contain at least one hospital?</p> <p>3) In Louisiana (STATEFP 22), what is the maximum Insurance payout amount (in USD) for structural building damage across all census tracts that contain at least one hospital?</p>   | <p>1) spatial-filtered counting &amp; ranking</p> <p>2) spatial filter and attribute average computation</p> <p>3) spatial filter and max aggregation</p>     |
| L5    | 3           | Spatial-Spatial | <p>1) How many hospitals are located within both FEMA floodplain polygons and census tract boundaries in Harris County, Texas (identified by the leftmost 5 digits of GEOID 48201 in the census_tract table)?</p> <p>2) What is the average total intersection area between each census tract and FEMA floodplain polygons, considering only tracts that also intersect ZCTA geometries, in Palm Beach County, Florida (identified by the leftmost 5 digits of GEOID 12099 in the census_tract table)?</p> <p>3) What percentage of census tracts in Dallas County, Texas (identified by the leftmost 5 digits of GEOID 48113 in the census_tract table) intersect both FEMA floodplain polygons and county geometries?</p> | <p>1) multi-layer containment counting</p> <p>2) multi-layer intersection-area aggregation</p> <p>3) multi-criteria spatial percentage calculation</p>        |

Table 2: FLOODSQL-BENCH benchmark with example questions and their specific question types. The number of questions-SQL samples at each difficulty level, {L0, L1, L2, L3, L4, L5}={50, 100, 150, 50, 43, 50}, resulting in a total number of 443 question-SQL pairs.

tion constraints defined in the metadata. To ensure consistency and interpretability, SQL generation is restricted to a limited yet well-defined set of functions, each aligned with specific reasoning categories. Inspired by TableBench (Wu et al., 2025), we incorporate a voting-based validation mechanism in which multiple LLM agents assess the correctness of each generated query. We iteratively refine each question–SQL pair until all three agents reach consensus that the SQL is valid and constitutes a reasonable answer to the question. To further ensure quality, we execute every SQL query against the benchmark database to confirm that it runs successfully and produces a sensible output. Finally, although not illustrated in Figure 1, we perform an additional semantic consistency check in which human reviewers verify that each question faithfully reflects its corresponding SQL logic; any ambiguous or underspecified cases are manually revised for clarity.

## 4 Experiments

In this section, we evaluate recent LLM agents equipped with the same RAG framework and compare their performance in the flood-risk-analytics domain. Our benchmark spans various query types, including single-table reasoning, double-table key-based joins, double-table spatial joins, triple-table key–key joins, triple-table key–spatial joins, and triple-table spatial–spatial joins.

### 4.1 Evaluation Protocol

In geo-spatial text-to-SQL tasks, particularly those involving polygon layers, naively generated SQL queries often invoke expensive spatial operators, leading to long execution times. While human experts can manually design optimized SQL solutions that avoid such bottlenecks, LLM-based RAG systems frequently produce spatial joins or geometric operations that are too slow to execute in practice. A straightforward mitigation strategy is to impose a time threshold, but this approach is brittle because query latency varies significantly across hardware environments. To address this issue, we propose a non-execution-based evaluation method: we embed both the ground-truth SQL and the LLM-generated SQL using OpenAI text-embedding-3-large and Jina Embeddings v3, and compute the cosine similarity between the resulting vectors. This avoids executing potentially expensive geospatial SQL, while still providing a reliable proxy for semantic

similarity between candidate and reference queries.

### 4.2 RAG Framework

To support geospatial text-to-SQL generation in the flood-risk-analytics domain, we build a metadata-driven Retrieval-Augmented Generation (RAG) framework tailored to the structure of FLOODSQL-BENCH. As show in Fig. 2, the system performs multi-granularity retrieval, first at the table level, then at the column level, before constructing a structured metadata prompt for SQL generation.

**(1) Table catalog.** Each relational or geospatial layer is represented by a table-level description that concatenates the table name with all schema fields and their summaries. During inference, the natural-language question is embedded and compared against these descriptions using cosine similarity. We select the Top-K most relevant tables (with K=3 for single-table tasks, K=4 for double-table tasks, and K=5 for more complex multi-table queries). This step constrains the LLM to operate only over valid tables and mitigates hallucination.

**(2) Column-level descriptions.** For each selected table, we maintain a column-level index where every entry pairs a column name with its semantic description. After table retrieval, the question is embedded again and matched against the column index of each chosen table. We then select the Top-5 most relevant columns per table, providing the LLM with fine-grained grounding (e.g., tract identifiers, FIPS codes, polygon geometries). These retrieved entries help the model map linguistic cues in the question to the appropriate attributes.

**(3) Functional notes.** We include a global set of operational notes summarizing CRS conventions, geometry validity requirements, common preprocessing steps, and warnings about expensive spatial operations. These notes bias the model toward efficient and domain-appropriate SQL patterns, preventing common spatial-analytics errors.

**(4) Join rules.** Because FLOODSQL-BENCH spans heterogeneous data sources, we provide explicit join rules covering direct key-based joins, concatenated ID joins, polygon-polygon spatial intersections, and point-in-polygon containment relationships. Exposing these rules gives the model structural priors that greatly reduce invalid joins and guide it toward plausible execution plans.

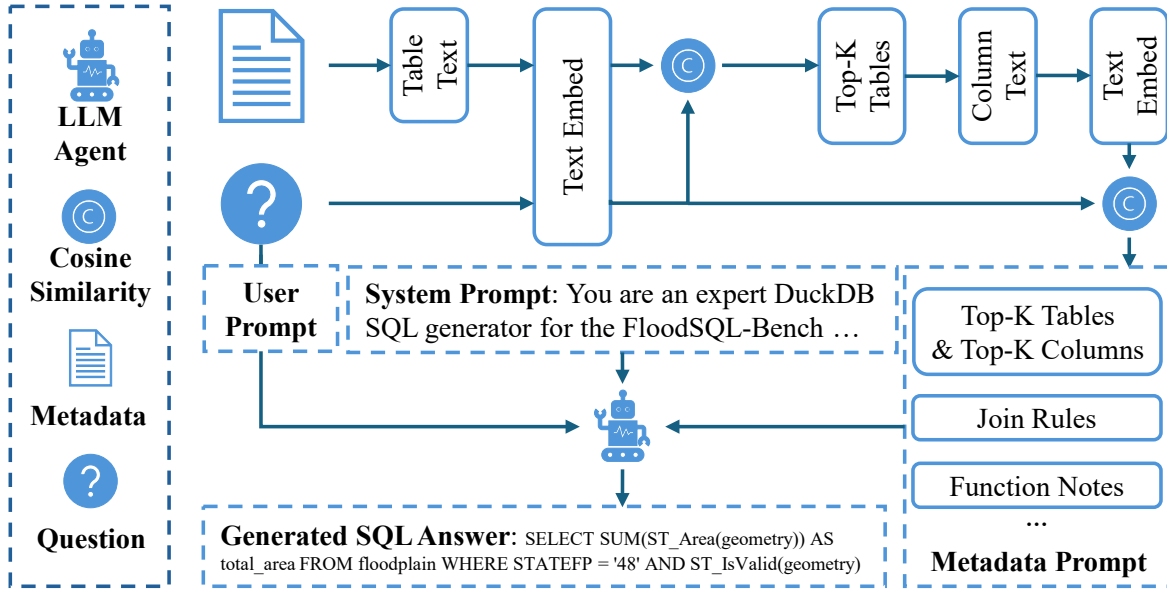


Figure 2: The Retrieval-Augmented Generation (RAG) architecture used to evaluate different LLM agents on FLOODSQL-BENCH. We compute text embeddings for both table-level and column-level metadata and measure their cosine similarity with the embedded question (user query) sequentially. The top-scoring tables and columns are selected as retrieved candidates for downstream SQL generation.

**Inference workflow.** Given a question, the system performs (i) dense table retrieval (Top-K), (ii) dense column retrieval for each selected table (Top-5), and (iii) metadata assembly that merges retrieved tables, selected attributes, functional notes, and join rules into a structured context. This enriched prompt is fed to the LLM, which is instructed to output exactly one DuckDB SQL query using only the retrieved tables and columns. This metadata-aligned RAG pipeline reduces ambiguity, improves schema grounding, and enhances the efficiency of generated geospatial SQL. **We use NULL to denote the failed SQL predictions.**

### 4.3 Results and Analysis

Table 3 summarizes the performance of more than twenty state-of-the-art LLMs equipped with the same retrieval-augmented (RAG) SQL generation pipelines on FLOODSQL-BENCH. Across all models, we observe that the proposed RAG framework, supported by metadata such as join rules, general notes, and function descriptions, consistently enables strong SQL generation performance, indicating the effectiveness of structured retrieval guidance for cross-table geospatial reasoning.

Among all closed-source LLM agents evaluated, Table 3 shows that GPT-4o and Claude-4.5-Opus demonstrates the strongest overall performance across all difficulty levels. More specifically, we observe that recent GPT models, includ-

ing GPT-4o, GPT-4.1, and GPT-5.1, exhibit consistent and comparable SQL generation performance on FLOODSQL-BENCH. A similar pattern holds for the Gemini family and Claude series. For example, models ranging from Gemini-2.0-Flash-Lite to Gemini-2.5-Pro show relatively stable performance across benchmark categories, and Claude models from Claude-3-Haiku to Claude-4.5-Opus likewise achieve closely aligned results.

Among all open-source LLM agents evaluated, DeepSeek-V3.2-685B demonstrates the strongest overall SQL generation capability under our proposed RAG framework. Within the DeepSeek family, DeepSeek-V3.2 achieves the highest overall performance across all categories. Other DeepSeek variants follow a clear scaling trend in which larger model sizes yield more accurate SQL predictions.

## 5 Conclusion

In this work, we presented FLOODSQL-BENCH, the first Text-to-SQL benchmark specifically designed for flood-risk analytics and multi-layer geospatial reasoning. By integrating real-world datasets spanning demographic, infrastructural, and floodplain information, the benchmark introduces progressively complex query types that require models to perform key-based joins, spatial joins, and hybrid multi-table reasoning. Our comprehensive evaluation across a broad set of proprietary and open-source LLMs, under a unified RAG frame-

| Model   | Level 0      |              | Level 1      |              | Level 2      |              | Level 3      |              | Level 4      |              | Level 5      |              |
|---|--------------|--------------|--------------|--------------|--------------|--------------|--------------|--------------|--------------|--------------|--------------|--------------|
|   | OpenAI       | Jina         |
| <b>Close-Source in Retrieval-Augmented SQL Generation Methods</b> |              |              |              |              |              |              |              |              |              |              |              |              |
| GPT-4o  | 0.914        | 0.962        | <b>0.891</b> | <b>0.957</b> | <u>0.909</u> | <b>0.974</b> | 0.883        | <u>0.951</u> | <b>0.904</b> | <b>0.962</b> | 0.919        | <b>0.976</b> |
| GPT-4.1   | 0.915        | 0.951        | 0.876        | 0.945        | 0.897        | 0.966        | 0.864        | 0.938        | 0.877        | 0.945        | 0.907        | 0.964        |
| GPT-5.1   | 0.917        | <u>0.963</u> | 0.886        | <u>0.953</u> | 0.899        | <u>0.970</u> | 0.863        | 0.945        | 0.895        | 0.955        | 0.910        | 0.968        |
| Gemini-2.0-Flash-Lite*  | 0.897        | 0.934        | 0.869        | 0.945        | 0.907        | 0.962        | 0.885        | 0.948        | –            | –            | 0.914        | 0.964        |
| Gemini-2.5-Flash-Lite   | 0.885        | 0.945        | 0.846        | 0.934        | 0.906        | 0.967        | 0.855        | 0.937        | 0.872        | 0.943        | 0.901        | 0.958        |
| Gemini-2.5-Pro  | 0.887        | 0.943        | 0.872        | 0.952        | <b>0.914</b> | <b>0.974</b> | 0.862        | 0.940        | 0.883        | 0.955        | 0.923        | 0.970        |
| Claude-3-Haiku  | <u>0.919</u> | 0.957        | 0.862        | 0.939        | 0.895        | 0.960        | 0.870        | 0.947        | 0.895        | 0.957        | 0.895        | 0.960        |
| Claude-3.5-Haiku  | 0.903        | 0.949        | 0.851        | 0.934        | 0.899        | 0.969        | 0.833        | 0.933        | <u>0.898</u> | <u>0.961</u> | 0.899        | 0.966        |
| Claude-4.5-Haiku*   | –            | –            | 0.870        | 0.938        | 0.896        | 0.966        | 0.879        | 0.949        | 0.895        | 0.958        | 0.921        | 0.973        |
| Claude-4.5-Sonnet   | 0.907        | 0.950        | 0.856        | 0.931        | 0.904        | 0.969        | 0.890        | <u>0.951</u> | <b>0.904</b> | 0.952        | <u>0.924</u> | 0.965        |
| Claude-4.5-Opus   | <b>0.923</b> | <b>0.965</b> | <u>0.889</u> | 0.951        | <u>0.909</u> | <b>0.974</b> | <b>0.899</b> | <b>0.955</b> | –            | –            | <b>0.931</b> | <u>0.974</u> |
| <b>Open-Source in Retrieval-Augmented SQL Generation Methods</b>  |              |              |              |              |              |              |              |              |              |              |              |              |
| Deepseek-R1-7B*   | 0.732        | 0.766        | –            | –            | 0.752        | 0.812        | –            | –            | 0.776        | 0.843        | 0.777        | 0.812        |
| Deepseek-R1-14B*  | 0.802        | 0.868        | 0.792        | 0.888        | –            | –            | 0.765        | 0.853        | 0.803        | 0.882        | 0.826        | 0.886        |
| Deepseek-R1-32B*  | <b>0.848</b> | 0.903        | 0.843        | 0.925        | 0.887        | 0.961        | –            | –            | 0.889        | <u>0.958</u> | 0.912        | <b>0.971</b> |
| Deepseek-V3.2-685B  | <b>0.908</b> | <b>0.949</b> | <u>0.873</u> | <b>0.949</b> | <b>0.908</b> | <u>0.963</u> | <b>0.888</b> | <b>0.948</b> | <u>0.896</u> | <u>0.958</u> | <b>0.924</b> | <b>0.971</b> |
| Qwen3-1.7B  | 0.861        | 0.916        | <u>0.827</u> | 0.910        | 0.846        | <u>0.924</u> | 0.793        | 0.886        | <u>0.824</u> | <u>0.900</u> | 0.856        | 0.926        |
| Qwen3-8B  | 0.903        | 0.936        | 0.862        | 0.940        | <u>0.904</u> | 0.961        | 0.871        | 0.942        | 0.875        | 0.946        | 0.912        | 0.967        |
| Qwen3-14B   | 0.895        | 0.933        | 0.864        | 0.940        | 0.893        | <u>0.963</u> | 0.869        | 0.938        | 0.888        | 0.957        | 0.910        | <u>0.970</u> |
| Qwen3-32B   | 0.896        | 0.935        | 0.859        | 0.937        | 0.902        | <u>0.962</u> | <u>0.873</u> | 0.943        | 0.893        | 0.957        | <u>0.918</u> | <b>0.971</b> |
| Qwen3-235B-A22B   | 0.894        | 0.942        | <b>0.877</b> | <u>0.946</u> | 0.891        | <b>0.964</b> | 0.867        | <u>0.947</u> | <b>0.898</b> | <b>0.962</b> | 0.916        | <b>0.971</b> |
| Gemma-2-2B*   | 0.879        | 0.931        | 0.820        | 0.907        | –            | –            | 0.841        | 0.919        | 0.818        | 0.909        | 0.851        | 0.924        |
| Gemma-2-9B  | <u>0.904</u> | <u>0.944</u> | 0.865        | 0.942        | <u>0.904</u> | 0.958        | 0.859        | 0.934        | 0.877        | 0.948        | 0.914        | 0.964        |

Table 3: Cosine similarity scores between predicted SQL results and gold SQL answers across the six benchmark task types: single-table reasoning (level 0); double-table key joins (level 1); double-table spatial joins (level 2); triple-table key–key joins (level 3); triple-table key–spatial joins (level 4); and triple-table spatial–spatial joins (level 5). For each task type, we report scores computed with **OpenAI text-embedding-3-large** (OpenAI) and **Jina Embeddings v3** (Jina). All nine LLM–RAG agents are evaluated under the same RAG SQL generation framework as shown in Fig. 2. The best results are **bold** while the second best results are underlined. \* marks LLM agents that exhibited timeouts or failure cases during SQL generation due to computation limitations. Following a best-effort validation process, any invalid or incomplete SQL outputs were removed from evaluation, denoted as –.

work, reveals that with appropriate retrieval settings and metadata hints, model performance on more challenging spatial and multi-table queries can approach that of simple single-table tasks. FLOODSQL-BENCH enables more robust evaluation, fosters the development of specialized methods, and ultimately supports more reliable decision-making in flood management and related geospatial domains. Our benchmark will be open-sourced.

## Limitations

This is the section for limitations

## Acknowledgments

This is the section for acknowledgments

## References

Orlando Ayala and Patrice Bechard. 2024. Reducing hallucination in structured outputs via retrieval-augmented generation. In *Proceedings of the 2024*

*Conference of the North American Chapter of the Association for Computational Linguistics: Human Language Technologies (Volume 6: Industry Track)*, pages 228–238.

Peter A Burrough, Rachael A McDonnell, and Christopher D Lloyd. 2015. *Principles of geographical information systems*. Oxford university press.

CDC/ATSDR. 2022. Social vulnerability index (svi). <https://www.atsdr.cdc.gov/place-health/php/svi/>.

Jiaqi Chen, Jianheng Tang, Jinghui Qin, Xiaodan Liang, Lingbo Liu, Eric Xing, and Liang Lin. 2021. Geoqa: A geometric question answering benchmark towards multimodal numerical reasoning. In *Findings of the Association for Computational Linguistics: ACL-IJCNLP 2021*, pages 513–523.

Susan L Cutter, Bryan J Boruff, and W Lynn Shirley. 2012. Social vulnerability to environmental hazards. In *Hazards vulnerability and environmental justice*, pages 115–132. Routledge.

FEMA. 2025. Openfema datasets and national flood hazard layer (nfh). <https://hazards.fema.gov>.

- GEOS Development Team. *Geos: Geometry engine, open source*. Accessed: 2025-10-01.
- Michael F Goodchild. 1992. Geographical information science. *International journal of geographical information systems*, 6(1):31–45.
- HIFLD. 2024. Hospitals and public schools. <https://www.dhs.gov/gmo/hifld>.
- Gautier Izacard and Edouard Grave. 2021. Leveraging passage retrieval with generative models for open domain question answering. In *Proceedings of the 16th conference of the european chapter of the association for computational linguistics: main volume*, pages 874–880.
- George Katsogiannis-Meimarakis and Georgia Koutrika. 2023. A survey on deep learning approaches for text-to-sql. *The VLDB Journal*, 32(4):905–936.
- Patrick Lewis, Ethan Perez, Aleksandra Piktus, Fabio Petroni, Vladimir Karpukhin, Naman Goyal, Heinrich Küttler, Mike Lewis, Wen-tau Yih, Tim Rocktäschel, and 1 others. 2020. Retrieval-augmented generation for knowledge-intensive nlp tasks. *Advances in neural information processing systems*, 33:9459–9474.
- Hao Li, Peng Yue, Haoru Wu, Baoxin Teng, Yongkun Zhao, and Changfeng Liu. 2025. A question-answering framework for geospatial data retrieval enhanced by a knowledge graph and large language models. *International Journal of Digital Earth*, 18(1):2510566.
- Jingjing Li, Wenlu Wang, Wei-Shinn Ku, Yingtao Tian, and Haixun Wang. 2019. Spatialnli: A spatial domain natural language interface to databases using spatial comprehension. In *Proceedings of the 27th ACM SIGSPATIAL International Conference on Advances in Geographic Information Systems*, pages 339–348.
- Jinyang Li, Binyuan Hui, Ge Qu, Jiayi Yang, Binhua Li, Bowen Li, Bailin Wang, Bowen Qin, Ruiying Geng, Nan Huo, and 1 others. 2023. Can llm already serve as a database interface? a big bench for large-scale database grounded text-to-sqls. *Advances in Neural Information Processing Systems*, 36:42330–42357.
- Mengyi Liu, Xieyang Wang, Jianqiu Xu, Hua Lu, and Yongxin Tong. 2025. Nalspatial: A natural language interface for spatial databases. *IEEE Transactions on Knowledge and Data Engineering*.
- Kurt Shuster, Spencer Poff, Moya Chen, Douwe Kiela, and Jason Weston. 2021. Retrieval augmentation reduces hallucination in conversation. *arXiv preprint arXiv:2104.07567*.
- U.S. Census Bureau. 2020. Geographic identifiers (geoids). <https://www.census.gov/programs-surveys/geography/guidance/geo-identifiers.html>. Accessed: 2025-11-05.
- U.S. Census Bureau. 2024. Tiger/line shapefiles and community resilience estimates. <https://www.census.gov>.
- Maheswari Visvalingam and James D Whyatt. 2017. Line generalization by repeated elimination of points. In *Landmarks in Mapping*, pages 144–155. Routledge.
- Oliver EJ Wing, Paul D Bates, Andrew M Smith, Christopher C Sampson, Kris A Johnson, Joseph Fargione, and Philip Morefield. 2018. Estimates of present and future flood risk in the conterminous united states. *Environmental Research Letters*, 13(3):034023.
- Shirley Wu, Shiyu Zhao, Michihiro Yasunaga, Kexin Huang, Kaidi Cao, Qian Huang, Vassilis N Ioannidis, Karthik Subbian, James Zou, and Jure Leskovec. 2024. Stark: Benchmarking llm retrieval on textual and relational knowledge bases. *Advances in Neural Information Processing Systems*, 37:127129–127153.
- Xianjie Wu, Jian Yang, Linzheng Chai, Ge Zhang, Jiaheng Liu, Xeron Du, Di Liang, Daixin Shu, Xi-anfu Cheng, Tianzhen Sun, and 1 others. 2025. Tablebench: A comprehensive and complex benchmark for table question answering. In *Proceedings of the AAAI Conference on Artificial Intelligence*, volume 39, pages 25497–25506.
- Tao Yu, Rui Zhang, Heyang Er, Suyi Li, Eric Xue, Bo Pang, Xi Victoria Lin, Yi Chern Tan, Tianze Shi, Zihan Li, and 1 others. 2019a. Cosql: A conversational text-to-sql challenge towards cross-domain natural language interfaces to databases. In *Proceedings of the 2019 conference on empirical methods in natural language processing and the 9th international joint conference on natural language processing (EMNLP-IJCNLP)*, pages 1962–1979.
- Tao Yu, Rui Zhang, Kai Yang, Michihiro Yasunaga, Dongxu Wang, Zifan Li, James Ma, Irene Li, Qingning Yao, Shanelle Roman, and 1 others. 2018. Spider: A large-scale human-labeled dataset for complex and cross-domain semantic parsing and text-to-sql task. *arXiv preprint arXiv:1809.08887*.
- Tao Yu, Rui Zhang, Michihiro Yasunaga, Yi Chern Tan, Xi Victoria Lin, Suyi Li, Heyang Er, Irene Li, Bo Pang, Tao Chen, and 1 others. 2019b. Sparc: Cross-domain semantic parsing in context. *arXiv preprint arXiv:1906.02285*.
- Kun Zhang, Xiexiong Lin, Yuanzhuo Wang, Xin Zhang, Fei Sun, Cen Jianhe, Hexiang Tan, Xuhui Jiang, and Huawei Shen. 2023. Refsql: A retrieval-augmentation framework for text-to-sql generation. In *Findings of the Association for Computational Linguistics: EMNLP 2023*, pages 664–673.
- Yifan Zhang, Cheng Wei, Zhengting He, and Wenhao Yu. 2024. Geogpt: An assistant for understanding and processing geospatial tasks. *International Journal of Applied Earth Observation and Geoinformation*, 131:103976.

Angelo Ziletti and Leonardo D'Ambrosi. 2024. Retrieval augmented text-to-sql generation for epidemiological question answering using electronic health records. In *Proceedings of the 6th Clinical Natural Language Processing Workshop*, pages 47–53.

## A Dataset Details

If there is any discrepancy between the released benchmark and this paper. Please follow the latest released benchmark.

### A.1 Spatial Details

**Geometries and preprocessing.** We standardize geometries to OGC:CRS84 (WGS84 lon/lat, degrees). Polygon geometries are retained for floodplain, census\_tracts, zcta, and county; claims are stored as point geometries (WKB). In contrast, schools and hospitals are represented by explicit LAT/LON fields (their opaque point BLOBs are discarded), and points are constructed on demand via `ST_Point(LON, LAT)`. Floodplain, tract, ZCTA, and county polygons together contain nearly one million geometries and hundreds of millions of vertices. To ensure query efficiency, we apply topology-preserving simplification (`ST_SimplifyPreserveTopology`) with dataset-specific tolerances,  $10^{-3}$  ( $\approx 100\text{m}$ ) for floodplains,  $10^{-4}$  ( $\approx 10\text{m}$ ) for tracts, and  $5 \times 10^{-4}$  ( $\approx 50\text{m}$ ) for ZCTAs and counties, only on polygons with  $>1\text{K}$ – $2\text{K}$  vertices, reducing vertex counts by 40–80% without altering query semantics. Table 4 reports this reduction quantitatively.

**Point vs. polygon data.** FloodSQL\_Bench distinguishes polygon-based from point-based layers. Polygon tables (census\_tracts, floodplain, zcta, county) retain geometries for overlay operations. Point-based tables differ: schools and hospitals rely solely on explicit LAT/LON fields, with points constructed on demand (`ST_Point(LON, LAT)`). Point datasets (claims, schools, hospitals) are consistently treated as explicit latitude/longitude pairs, with geometries constructed on demand. claim geometry is kept in the schema but used only for key-based aggregation via GEOID identifiers. The claims table functions as a key-joinable layer rather than a spatially joined one, enabling direct integration with tract-level indicators (e.g., NRI, SVI, CRE) via 11-digit GEOIDs. This design makes spatial joins explicit and keeps geometry handling transparent for LLMs.

### A.2 Value Summary of Tables

As shown in Table 5-14, we provide column statistics and example values for each table in FloodSQL\_Bench. For numeric columns we show the value range; for categorical or string columns

we show the number of unique values and sample examples. For clarity, we omit raw geometry BLOB columns from the value summary tables. These columns exist in the following datasets: census\_tracts, claims, county, floodplain, and zcta.

### A.3 Detailed Join Rules by Table

We provide a per-table summary of how each dataset in FloodSQL\_Bench participates in join operations. This complements the join matrix Table 1.

- **county:** County-level administrative polygon layer representing U.S. counties. Each record corresponds to a single county area within a state. This table supports both key-based joins via the 5-digit GEOID and spatial joins via the geometry field.
- **census\_tracts:** Polygon-based spatial layer representing U.S. Census tracts. Each record corresponds to a single tract area defined by the U.S. Census Bureau. This table supports key-based joins via the 11-digit GEOID and spatial joins with polygon-based layers and point-based layers through its geometry field.
- **claims:** Key-based table containing National Flood Insurance Program (NFIP) flood claim records. Each record represents a single insurance claim event linked to a census tract. All joins are key-based using the 11-digit GEOID; spatial joins are not applicable.
- **floodplain:** FEMA Flood Hazard polygon layer representing physical flood risk zones. Each record corresponds to a FEMA-defined flood hazard area. This table is spatial-only and supports spatial joins through its geometry field, but is not used for key-based joins.
- **zcta:** ZIP Code Tabulation Area (ZCTA) polygon layer representing U.S. postal ZIP code regions. ZCTAs are spatial constructs derived from census data and are not identical to USPS ZIP codes. This table supports spatial joins via its geometry field but is not used for key-based joins.
- **schools:** Point-based layer representing school facilities across Texas, Florida, and Louisiana. Each record corresponds to one educational institution, including colleges, private, and public schools. This table

| Dataset       | Rows    | Points (Before) | Points (After) | Avg pts (Before) | Avg pts (After) |
|---------------|---------|-----------------|----------------|------------------|-----------------|
| Floodplain    | 915,760 | 734,284,445     | 179,571,368    | 801.8            | 196.1           |
| Census tracts | 13,444  | 5,474,058       | 3,279,789      | 407.2            | 244.0           |
| ZCTA          | 5,284   | 8,583,835       | 1,825,650      | 1624.5           | 345.5           |

Table 4: Comparison of geometry statistics before and after simplification. Row counts are preserved while point counts are significantly reduced, improving query efficiency in FloodSQL\_Bench.

| Column   | Summary  |
|----------|--|
| GEOID    | 13,444 unique; e.g., 12011010102, 12011110402, 12011010304 |
| STATEFP  | 3 unique; examples: 12                                     |
| COUNTYFP | 255 unique; examples: 011, 099                             |
| NAME     | 8,048 unique; examples: 101.02, 1104.02                    |

Table 5: Value summary for census\_tracts\_tx\_fl\_la.

| Column                                     | Summary                                       |
|--|---|
| GEOID                                      | 12,756 unique; e.g., 12086000709, 48167723505 |
| STATEFP                                    | 3 unique; examples: 12, 22, 48                |
| dateOfLoss                                 | 15,042 unique dates                           |
| amountPaidOnBuildingClaim                  | range: -201,667.50 .. 10,741,476.93           |
| amountPaidOnContentsClaim                  | range: -80,000.00 .. 500,000.00               |
| amountPaidOnIncreasedCostOfComplianceClaim | range: -6,450.00 .. 426,321.00                |

Table 6: Value summary for claims\_tx\_fl\_la.

| Column   | Summary                                   |
|----------|---|
| GEOID    | 385 unique; e.g., 48327, 48189            |
| STATEFP  | 3 unique; examples: 12, 22, 48            |
| COUNTYFP | 255 unique; e.g., 327, 189, 011           |
| NAME     | 357 unique; e.g., Menard, Hale, Armstrong |

Table 7: Value summary for county\_tx\_fl\_la.

| Column   | Summary                                  |
|----------|--|
| GFID     | 199 unique; e.g., 20120202, 20110720LOMR |
| STATEFP  | 3 unique; examples: 12, 22, 48           |
| FLD_ZONE | 10 unique; e.g., A, AE, X, D             |

Table 8: Value summary for floodplain\_tx\_fl\_la.

| Column  | Summary                                 |
|---------|---|
| GEOID   | 5,284 unique; e.g., 34210, 33010, 33919 |
| STATEFP | 3 unique; examples: 12, 22, 48          |

Table 9: Value summary for zcta\_tx\_fl\_la.

| Column      | Summary  |
|-------------|--|
| HOSPITAL_ID | 1,526 unique; e.g., 0005479830, 0019879735                                 |
| NAME        | 1,508 unique; e.g., BIG BEND REGIONAL MEDICAL CENTER                       |
| ADDRESS     | 1,511 unique; e.g., 2600 HIGHWAY 118 NORTH                                 |
| CITY        | 566 unique; e.g., EL PASO, MIAMI, HOUSTON                                  |
| STATE       | 3 unique; TX, FL, LA   |
| ZIP         | 896 unique; e.g., 79912, 33177   |
| COUNTY      | 287 unique; e.g., EL PASO, MIAMI-DADE                                      |
| COUNTYFIPS  | 306 unique; e.g., 48141, 12086   |
| LAT         | range: 24.5641986 .. 36.36988585   |
| LON         | range: -106.5735232 .. -80.05188127  |
| TYPE        | 10 categories; e.g., GENERAL ACUTE CARE, CRITICAL ACCESS, PSYCHI-<br>ATRIC |
| STATEFP     | 3 unique; 12, 22, 48   |
| UNIQUE_ID   | 1,526 unique; e.g., 48_hospital_0005479830                                 |

Table 10: Value summary for hospitals\_tx\_fl\_la.

| Column    | Summary  |
|-----------|--|
| SCHOOL_ID | 19,669 unique; e.g., 476540, 488332, 226107              |
| NAME      | 17,947 unique; e.g., UNIVERSITY OF NORTH TEXAS AT DALLAS |
| ADDRESS   | 18,299 unique; e.g., 7300 UNIVERSITY HILLS DRIVE         |
| CITY      | 1,863 unique; e.g., DALLAS, MIAMI, HOUSTON               |
| STATE     | 3 unique; TX, FL, LA                                     |
| ZIP       | 2,874 unique; e.g., 75241, 33156                         |
| LAT       | range: 24.552411 .. 36.49455370700008                    |
| LON       | range: -106.62416140199996 .. -80.03827100000001         |
| TYPE      | 3 categories; COLLEGE, PUBLIC_SCHOOL, PRIVATE_SCHOOL     |
| STATEFP   | 3 unique; 12, 22, 48                                     |
| UNIQUE_ID | 19,669 unique; e.g., 48_COLLEGE_476540                   |

Table 11: Value summary for schools\_tx\_fl\_la.

| Column               | Summary  |
|----------------------|--|
| GEOID                | 13,385 unique; e.g., 12001000201, 12001000202                                    |
| ST / STATE / ST_ABBR | ST range: 12 .. 48; STATE: {Florida, Louisiana, Texas}; ST_ABBR: {FL,<br>LA, TX} |
| COUNTY               | 368 unique; e.g., Harris County, Miami-Dade County                               |
| FIPS                 | range: 12001000201 .. 48507950302  |
| AREA_SQMI            | range: 0.0 .. 6,175.6501   |
| E_TOTPOP             | range: 0 .. 28,999   |
| E_POV150             | range: 0 .. 7,002  |
| E_UNEMP              | range: 0 .. 915  |
| E_AGE65 / E_AGE17    | range: 0 .. 9,894 / 0 .. 10,142  |
| E_MINRTY             | range: 0 .. 21,476   |
| E_MUNIT / E_MOBILE   | range: 0 .. 6,733 / 0 .. 3,027   |
| EP_* (percentages)   | many in [-999, 100]; note: -999 denotes missing per SVI convention               |
| RPL_THEMES           | range: -999 .. 1.0 (percentile ranks with sentinel -999)                         |

Table 12: Selected indicators and ranges for svi\_tx\_fl\_la. (-999 indicates missing values per SVI specification.)

| <b>Column</b> | <b>Summary</b>  |
|---------------|---|
| GEOID         | 13,373 unique; e.g., 12001000201, 12001000202   |
| STATE         | 3 unique; FL, LA, TX  |
| RFLD_RISKR    | 7 categories; e.g., Very Low, Relatively Low, Relatively Moderate, Relatively High, Very High, No Rating, Insufficient Data |
| RFLD_EALB     | range: 0.0 .. 27,794,853.10   |
| RFLD_EALS     | range: 0.0 .. 99.99   |

Table 13: Selected value summary for nri\_tx\_fl\_la.

| <b>Column</b> | <b>Summary</b>  |
|---------------|---|
| GEOID         | 13,444 unique; e.g., 12001000201, 12001000202                   |
| GEO_ID        | 13,444 unique; e.g., 1400000US12001000201                       |
| STATE         | range: 12 .. 48   |
| COUNTY        | range: 1 .. 507   |
| TRACT         | range: 100 .. 990200  |
| NAME          | 13,444 unique; e.g., Census Tract 3.01, Alachua County, Florida |
| POPUNI        | range: 0 .. 31,221  |
| PRED0_E       | range: 0 .. 15,380  |
| PRED0_PE      | range: 0.0 .. 100.0   |
| PRED12_E      | range: 0 .. 15,470  |
| PRED12_PE     | range: 0.0 .. 100.0   |
| PRED3_E       | range: 0 .. 5,691   |
| PRED3_PE      | range: 0.0 .. 67.38   |

Table 14: Selected value summary for cre\_tx\_fl\_la.

supports spatial joins through coordinates (LON, LAT) for point-in-polygon operations with polygon layers. ZIP serves as the primary key for key-based joins with hospitals. Geometry can be constructed dynamically using ST\_Point(LON, LAT) in WGS84 (EPSG:4326)."

- **hospitals:** Point-based layer representing hospital facilities across Texas, Florida, and Louisiana. Each record corresponds to a single healthcare facility. This table supports both spatial joins through coordinates (LON, LAT) and key-based joins with schools via ZIP, with county-level and tract-level datasets via the 5-digit COUNTYFIPS code. Geometry can be constructed dynamically using ST\_Point(LON, LAT) in WGS84 (EPSG:4326).
- **SVI:** Key-based table representing the Social Vulnerability Index (SVI) dataset published by the CDC/ATSDR. Provides tract-level demographic, socioeconomic, housing, and mobility indicators used to measure a community's vulnerability to natural hazards and disasters. This dataset contains no geometry field; all joins are key-based via the 11-digit census tract GEOID. A FIPS field identical to GEOID exists in the source data, but GEOID is used as the canonical key in FloodSQL-Bench."
- **CRE:** Key-based table representing the Community Resilience Estimates (CRE) dataset published by the U.S. Census Bureau. Provides tract-level measures of population resilience to natural hazards, estimating how well communities can withstand and recover from disasters. This dataset contains no geometry field; all joins are key-based via the 11-digit census tract GEOID.
- **NRI:** Key-based table representing the National Risk Index (NRI) dataset developed by FEMA. Provides tract-level estimates of natural hazard risk across the United States, quantifying expected losses, exposure, and composite risk scores for multiple hazard types, including Coastal Flood (CFLD) and Riverine Flood (RFLD). This dataset contains no geometry field; all joins are key-based via the 11-digit census tract GEOID.